LBL-32473
UC-404

Lawrence Berkeley Laboratory
UNIVERSITY OF CALIFORNIA

CHEMICAL SCIENCES DIVISION

To be presented at the Rare Earths 1992 Conference, Kyoto, Japan, June 1-5, 1992, and to be published in the Proceedings

Spectroscopic and Magnetic Studies of Tetravalent Pa and Trivalent Th Compounds

N.M. Edelstein and W.K. Kot

June 1992

Prepared for the U.S. Department of Energy under Contract Number DE-AC03-76SF00098

DISCLAIMER

LBL-32473

Spectroscopic and Magnetic Studies of Tetravalent Pa and Trivalent Th Compounds

Norman M. Edelstein

Wing K. Kot

Chemical Sciences Division

Lawrence Berkeley Laboratory

University of California, Berkeley, CA 94720 U.S.A.

This work was supported by the Director, Office of Energy Research, Office of Basic Energy Sciences, Chemical Sciences Division of the U.S. Department of Energy under Contract No. DE-AC03-76SF00098.

Spectroscopic and Magnetic Studies of Tetravalent Pa and Trivalent Th Compounds

Norman M. Edelstein

Wing K. Kot

Chemical Sciences Division

Lawrence Berkeley Laboratory

University of California, Berkeley, CA 94720 U.S.A.

Abstract

At the beginning of the actinide series, the 5f and 6d configurations are very close in energy. Consequently, both the 5f and 6d energy level splittings may be observed experimentally in Pa^{4+} and Th^{3+} compounds. The available magnetic and optical data on these systems are reviewed.

Introduction

Before 1940, the elements Th, Pa, and U (atomic numbers 90-92) were placed below their 5d counterparts Hf, Ta, and W (atomic numbers 72-74) in the Periodic Table because of the similarity of their chemical properties to those 5d elements. However it had long been predicted theoretically that a new transition series should begin somewhere around uranium in the Periodic Table, and many early studies suggested this shell should consist of 5f electrons [1]. Today it

is known experimentally that the first appearance of 5f electrons in the free gaseous atoms of the present-day actinide series occurs at element 91, Pa, whose ground configuration is $5f^26d7s^2$ outside the closed radon shell. For all the early actinide gaseous atoms and ions, there are a number of low-lying electron configurations [2]. Placing these ions in compounds or crystals, can cause perturbations to the relative energies of these configurations due to the effects of the crystal field. The most noteable example is for the one structurally characterized compound of trivalent Th, $Cp_3"Th$ ($Cp" = \eta^5\text{-}C_5H_3\text{-}(SiMe_3)_2$) [3]. In the free trivalent Th ion, the lowest configuration is $5f^1$ with the $6d^1$ configuration starting at 9192.84 cm^{-1}. In $Cp_3"Th$, the ground configuration is $6d^1$ with the $5f^1$ configuration beginning at 15,350 cm^{-1}. Thus placing the Th^{3+} ion into this compound results in a stabilization of the lowest 6d energy level by greater than 24,000 cm^{-1}. Similar, though less dramatic, effects occur in Pa compounds. In this paper, electronic and magnetic studies on Pa^{4+} and Th^{3+} compounds will be reviewed.

Pa^{4+} Magnetism and Spectroscopy

The near infra-red spectrum of Pa^{4+} ($5f^1$) diluted into the host crystal Cs_2ZrCl_6 was measured originally by Axe [4]. He and coworkers also reported the EPR (electron paramagnetic resonance) spectrum of the ground state [5]. Pa^{4+} in this crystal is at a site of O_h symmetry and the energy level scheme is shown in Fig. 1. As will be discussed later it is appropriate to think of the active species as the

$PaCl_6^{2-}$ anion. Axe was the first to use Cs_2ZrCl_6 as a host crystal and this crystal has now been studied extensively with U^{4+} as the dopant ion [6], as well as with the Np^{4+} ion [7]. Axe also observed strong transitions in the visible region but did not give these bands a definite assignment.

The optical and magnetic data for Pa^{4+}/Cs_2ZrCl_6 were analyzed in terms of the crystal and spin-orbit interactions for an f^1 electron. The Hamiltonian for the energy levels of an f electron in octahedral symmetry may be written as

$$\mathcal{H} = \mathcal{H}_{SO} + \mathcal{H}_{CF}$$

$$\mathcal{H}_{SO} = \zeta_{\ell}(r)\boldsymbol{\ell}\cdot\boldsymbol{s}, \quad (1)$$

$$\mathcal{H}_{CF} = B_0^4[C_0^4 + (\tfrac{5}{14})^{1/2}(C_{-4}^4 + C_4^4)] + B_0^6[C_0^6 - (\tfrac{7}{2})^{1/2}(C_{-4}^6 + C_4^6)].$$

The effects due to the radial part of the 5f wavefunctions are contained in the crystal field parameters B_0^4 and B_0^6, and the spin-orbit coupling constant $\zeta_{5f}(r)$, which are evaluated empirically. The matrix elements for the angular momentum operators, $\boldsymbol{s}$ and $\boldsymbol{\ell}$, and the tensor operators, C_q^k, depend only on the angular coordinates and are evaluated by standard techniques [8].

Under the effect of the octahedral crystal field at the Pa^{4+} site, the seven degenerate f orbitals (of the free ion) decompose into two triplet states, t_{1u} and t_{2u}, and one singlet state, a_{2u} (O_h point group). When the electron spin is considered, each orbital becomes doubly degenerate and the double group representations Γ_{6u}, Γ_{7u}, and Γ_{8u} become the proper labels for the eigenstates and energy levels. Because the spin-

orbit coupling interaction is large compared to the crystal field interaction, the crystal field levels fall in two groups which can be described (approximately) by the term labels $^2F_{5/2}$ and $^2F_{7/2}$ (Fig. 1).

Although the 5f radial wavefunction is more extended than its 4f counterpart Ce^{3+}, it is still shielded from the surrounding environment by the $6s^2$ and $6p^6$ filled electron shells. The radial wavefunction of the 6d configuration extends significantly beyond the filled $6s^26p^6$ shells of the Rn core. Thus, the 6d electron experiences a crystal field that is much larger than the 6d spin-orbit coupling. The octahedral (O_h) crystal field of $PaCl_6^{2-}$ splits the 6d configuration into two levels, a t_{2g} lower state (triply degenerate) and an e_g upper state (doubly degenerate). When the 6d spin-orbit interaction is included, the t_{2g} level splits into a Γ_{8g} (a degenerate quartet with the inclusion of spin) state and a higher-lying Γ_{7g} (Kramers doublet) state. The higher-lying e_g level also transforms as a Γ_{8g} quartet when the spin-orbit coupling is considered (Fig. 1).

The EPR data can be fit with a spin-Hamiltonian of the form:

$$\mathcal{H} = g\,\beta\,\vec{H}\cdot\vec{S} + A\,\vec{I}\cdot\vec{S}. \qquad (2)$$

For the case of $^{231}Pa^{4+}/Cs_2ZrCl_6$, I (the nuclear spin) is equal to 3/2, and both g and A are isotropic because the ground state is a Γ_7 doublet (O_h symmetry). The values of ζ, B_0^4, B_0^6 and g, as obtained by Axe, et al. are given in Table 1 [5].

Additional near infra-red data have been reported for the pure hexahalocompounds at 85°K and room temperature [9,10]. These data were analyzed with the above model. The parameters and measured

values for two of the measured compounds, $(Et_4N)_2PaCl_6$ and $(Et_4N)_2PaF_6$, are also shown in Table 1.

Pa^{4+} diluted in single crystals of $ThBr_4$ and $ThCl_4$ has been thoroughly studied by near-infra-red emission and absorption spectroscopy and by EPR [11]. In addition, strong visible fluorescence in these crystals was observed and assigned to transitions from the $6d^1$ configuration to the 5f levels [12]. The $5f \rightarrow 6d$ absorption spectra of $Pa^{4+}/ThBr_4$ and of Pa^{4+} in solutions of the hexachloro- and hexabromo-salts also have been measured and analyzed [13].

Recently, visible fluorescence has been reported for the system, Pa^{4+}/Cs_2ZrCl_6 at 4.2K when excited with the 488 nm line of an argon ion laser [14]. This fluorescence arises from the lowest state in the $6d^1$ configuration ($6d\Gamma_{8g}$, see Fig. 1) to all five crystal field levels of the $5f^1$ configuration. The fluorescence shows highly structured sidebands with the most prominent feature arising from vibronic progressions of the 310 cm^{-1} totally symmetric stretching mode (ν_1) of the $PaCl_6^{2-}$ complex. Most of the other vibronic peaks can be assigned to even parity vibrations of the $PaCl_6^{2-}$ complex or the host lattice.

A study of the high-resolution absorption spectrum of Pa^{4+}/Cs_2ZrCl_6 has appeared [15]. Extensive vibrational structure was observed in the first 6d band ($6d\ \Gamma_{8g}$) and this structure has been compared with that found in the emission spectra. The emission spectra probe the details of the potential surface for the $5f^1$ configuration of the $PaCl_6^{2-}$ complex, while the absorption spectrum probes the potential surface of the $6d^1$ configuration. The major differences between the

absorption and the emission spectra were the absence of features due to e_g and t_{2g} normal modes in the absorption spectrum, and a very dramatic broadening of the higher energy vibronic features in the higher harmonics of the ν_1 vibration as shown in Fig. 2.

From the absorption spectrum of Pa^{4+}/Cs_2ZrCl_6, assignments have been made for the three 6d energy levels expected for a $6d^1$ electron in an O_h crystalline field. These levels are shown in Fig. 1 and tabulated in Table 1. The analyses of the energy levels of both the 6d and 5f configurations of Pa^{4+} in $ThBr_4$ and in Cs_2ZrCl_6 allow the change in the relative shifts of the centers of gravity of these two configurations to be compared with the free ion. This comparison is shown in Fig. 3, which also includes data for Ce^{3+} free ion ($4f^1$, $5d^1$) [16] and for Ce^{3+}/Cs_2NaYCl_6 [17,18]. Note these shifts in the relative energy difference between the d and the f configurations are approximately 17,400 cm^{-1} to 22,000 cm^{-1} for Pa^{4+} in the halide hosts, while it is approximately 14,400 cm^{-1} for Ce^{3+} in Cs_2NaYCl_6. Thus, extrapolating to the Th^{3+} free ion where the 6d configuration is only approximately 10,000 cm^{-1} above the 5f configuration in the free ion, the 6d configuration could plausibly be the ground configuration in Th^{3+} compounds.

From the data given in Table 1, the parameters of the Hamiltonian, Eq. 1, are overdetermined. The best fit parameters for Pa^{4+}/Cs_2ZrCl_6 are shown in Table 1. The crystal field parameters agree fairly well with those obtained from the analysis of the extensive experimental studies of U^{4+}/Cs_2ZrCl_6 ($5f^2$ configuration) [6]. Nevertheless, the simple crystal

field model is not adequate for the $5f^1$ system. For the analyses of the U^{4+}/Cs_2ZrCl_6 and U^{4+}/Cs_2ZrBr_6 systems ($5f^2$, in which the Slater parameters and the Trees parameter are included) Flint and Tanner report a root-mean-square (rms) deviation of ~150 cm^{-1} and greater for a large number of assigned levels [6]. Further calculations on the same energy levels sets using the parametric Hamiltonian as in the $UBD_4/HfBD_4$ study [19] did not significantly improve the fits [20]. These results are in contrast to analyses of other tetrapositive transprotactinium ion systems where the rms deviations are less than 100 cm^{-1} [21,22,23]. For the trivalent actinide ions in $LaCl_3$, the rms deviations are on the order of 18-22 cm^{-1} for most of the series [24]. However for $U^{3+}/LaCl_3$ the rms deivation was 29 cm^{-1} and Carnall has noted that the U^{3+} free ion parameters do not fit with the systematics of the rest of the series.

In general parametric fits for the tetravalent transuranium ions have an rms deviation greater than 35 cm^{-1}. The major difference between the trivalent and tetravalent ions in crystals or compounds is that the crystal field interaction is much larger for the latter series, especially in the host crystal, Cs_2ZrCl_6. There are a number of possibilities for the sources of these analysis problems at the beginning of both the trivalent and tetravalent actinide ion series. First of all, the 5f orbitals are most extended at the beginning of series which results in greater 5f-ligand interaction. Secondly, the $5f^{n-1}6d^1$ excited configuration is at its lowest relative energy in this region. Thus the parametric theory used to fit $5f^n$ optical spectra may be lacking

parameters which can take into account important interactions which occur at the beginning of the actinide series and the effects of a strong crystal field interaction.

Th^{3+} Magnetism and Spectroscopy

Although the energies of the low-lying configurations of the Th^{3+} free ion have been measured, almost nothing is known about the electronic structure of Th^{3+} in compounds. The one structurally characterized Th^{3+} compound, $Cp_3"Th$ has been shown to have a $6d^1$ ground state from EPR measurements as a function of temperature. The spectra are shown in Fig. 4. Recently Lukens and Andersen [25] have measured the EPR spectrum of Cp_3Zr where $Cp = \eta^5\text{-}C_5H_5$ (a $4d^1$ complex which is also assumed to have approximately D_{3h} symmetry) and its spin-Hamiltonian parameters are consistent with those of $Cp_3"Th$ when the much smaller spin-orbit coupling is considered. By contrast, the EPR spectrum of $Cp_3"Ce$ (a $4f^1$ complex with approximate D_{3h} symmetry) gives quite different values for the spin-Hamiltonian parameters and no room temperature spectrum is observed [26]. If D_{3h} symmetry about the Th^{3+} ion in $Cp_3"Th$ is assumed, the 6d orbitals will split into an orbital singlet A' and two orbital doublets, E' and E". The A' orbital (or $6d_z^2$) is lowest in energy because it most successfully avoids the electron density of the Cp rings. This assignment is the only consistent one with the observed EPR spectrum [3].

The complex Cp_3Th ($Cp = \eta^5\text{-}C_5H_5$) has also been reported previously. Kanellakopulos and coworkers reported a purple compound with a room temperature magnetic moment of 0.331 μ_B (μ_B

= Bohr magneton) and Marks and coworkers reported a green compound with $\mu_{eff} = 0.403\ \mu_B$ [27,28]. Photolysis of solutions of Cp_3ThR, $(MeCp)_3R$, and $(C_9H_7)_3ThR$ (MeCp = η^5-$C_5H_4CH_3$, C_9H_7 = η^5-$C_5H_3C_4H_4$) liberated gaseous alkanes and alkenes and the solutions became strongly colored [28]. Pulse radiolysis experiments on the compound $\eta^5(C_5Me_5)_2ThCl_2$ also produced a transient spectrum attributed to the species $(\eta^5\text{-}C_5Me)_2ThCl_2^-$ followed by a more stable species assigned to $(\eta^5\text{-}C_5Me_5)_2ThCl$. The latter species had an optical spectrum similar to the one obtained by the photolysis of a $(MeCp)_3Th$ alkyl attributed to $(\eta^5\text{-}C_5H_4Me)_3Th$ [29]. The room temperature optical spectrum of $Cp_3"Th$ is shown in Fig. 5. Three very strong bands are observed in the 15000-20000 cm^{-1} region along with a fourth peak at ~27000 cm^{-1} that overlaps a very broad absorption edge. Assuming D_{3h} symmetry, four allowed electric dipole transitions are expected from the ground 6d A_1' state to the 5f levels. It is expected the total span of the 5f configuration in Th^{3+} would be less than 6000 cm^{-1} (for Pa^{4+}/Cs_2ZrCl_6 it is ~8000 cm^1 with a larger spin-orbit coupling constant). Thus it is likely the fourth allowed 6d $\rightarrow$ 5f transition is masked by the three observed bands. The band at 27000 cm^{-1} is tentatively assigned as 6d $\rightarrow$ 7s or 7p [27].

Bursten and coworkers have carried out quasi-relativistic X-α SW calculations on the molecules Cp_3M (M = Th, Pa, U, Np, and Pu) [30]. Their results agree with the assigned $6d^1$ ground state for $Cp_3"Th$ (assuming Cp_3Th is similar to $Cp_3"Th$). Interestingly, Bursten, et al. point out the $6d_z^2$ orbital will be destabilized by the addition of a Lewis

base to a Cp_3Th molecule and predict for a hypothetical (to date) $Cp_3Th{\cdot}L$ molecule (C_{3v} symmetry about the Th^{3+} ion) a $5f^1$ ground state. They also predict the hypothetical Cp_3Pa molecule would have a $5f^16d^1$ ground state. Their calculations give approximately equal energies for the $5f^3$ and $5f^26d^1$ configurations for the molecule Cp_3U although experimental magnetic and optical data clearly indicate the ground state is $5f^3$ for $Cp_3"U$ with the start of the $5f^26d^1$ configuration greater than 20000 cm^{-1} [31].

Although no $Cp_3"Th{\cdot}L$ compounds (where L is a Lewis base) are known, the analogous $Cp_3"Ce$ and $Cp_3"Ce{\cdot}CN^tBu$ compounds have been synthesized and crystallographically characterized [32]. The symmetry about the Ce^{3+} ion in each compound is approximately D_{3h} and C_{3v}, respectively. For Ce^{3+} compounds the ground state is unequivocally $4f^1$ and the first 5d level can vary from ~20,000 to 40,000 cm^{-1} in energy depending on the ligands about the Ce^{3+} ion [33]. Measurements of the $4f \rightarrow 5d$ transitions for the two Ce^{3+} compounds given above show a shift of about 6000 cm^{-1} to higher energy for the first 5d level of $Cp_3"Ce{\cdot}L$ as compared to the base-free compound [26]. It is possible this effect might be considerably larger in the analogous Th complex.

EPR experiments have been performed on the photolysis product of $(C_9H_7)_3ThCH_3$. If the photolysis product (which is highly colored) is $(C_9H_7)_3Th$ and has the same structure as $(C_9H_7)_3U$, then this compound would have the pentahapto indenyl rings surrounding the Th^{3+} ion in a trigonal manner [34]. Thus the electronic structure should

be similar to that of $Cp_3"Th$. A room temperature EPR signal was observed upon photolysis with a g value of 1.953. Measuring the frozen solution at 80K gave an axial spectrum consistent with a $6d^1$ configuration. Although the signal was weak due to the limited solubility of the $(C_9H_7)_3ThCH_3$ and the low quantum yield of the photolysis step, this experiment does confirm the assignment of the $6d^1$ configuration in these types of molecules [26].

Conclusion

At the beginning of both the actinide and lanthanide series, the 5f(4f) and 6d(5d) configurations are rather close in energy. Optical and EPR studies have been utilized to explore the relative energies of these two configurations. Does the unusual bonding of the early actinide ions arise from the extended nature of the 5f orbitals at the beginning of the series? Or does it arise from the relatively close proximity of the 6d configuration? Theoretical calculations on organometallic molecules do indicate the 6d orbitals play a dominant role [35]. More extensive studies on Th^{3+} and Pa^{4+} compounds may help in answering the above questions.

Acknowledgement.

This work was supported by the Director, Office of Energy Research, Office of Basic Energy Sciences, Chemical Sciences Division of the U.S. Department of Energy under Contract No. DE-AC03-76SF00098.

References

1. G.T. Seaborg in "The Comparative Science of the Actinide and Lanthanide Elements," G. Choppin, Ed., Elsevier, New York 1992.
2. M. Fred in "The Chemistry of the Actinide Elements," J.J. Katz, G.T. Seaborg, and L.R. Morss, Eds., Chapman and Hall, London, 1986, pp. 1196-1234.
3. W.K. Kot, G.V. Shalimoff, N.M. Edelstein, M.A. Edelman, and M.F. Lappert, J. Am. Chem. Soc. 110 (1988) 986.
4. J.D. Axe, "The Electronic Structure of Octahedrally Coordinated Protactinium(IV)," UCRL-9293, 1960.
5. J.D. Axe, H.J. Stapleton, and C.D. Jeffries, Phys. Rev. 121 (1961) 1630.
6. C.D. Flint and P.A. Tanner, Mol. Phys. 61 (1987) 389 and references given herein.
7. N. Edelstein, W. Kolbe, and J.E. Bray, Phys. Rev. B 21 (1980) 338 and references given herein.
8. B.G. Wybourne, "Spectroscopic Properties of Rare Earths," Wiley, New York, 1965.
9. N. Edelstein, D. Brown, and B. Whittaker, Inorg. Chem. 13 (1974) 563.
10. D. Brown, B. Whittaker, and N. Edelstein, Inorg. Chem. 13 (1974) 1805.
11. J.-C. Krupa, S. Hubert, M. Foyentin, E. Gamp, and N. Edelstein, J. Chem. Phys. 78 (1983) 2175.
12. R.C. Naik and J.-C. Krupa, J. Lumin. 31/32 (1984) 222.
13. N. Edelstein, J.-C. Krupa, R.C. Naik, K. Rajnak, B. Whittaker, and D. Brown, Inorg. Chem. 27 (1988) 3186.
14. D. Piehler, W.K. Kot, and N. Edelstein, J. Chem. Phys. 94 (1991) 942.

15. N. Edelstein, W.K. Kot, J.-C. Krupa, J. Chem. Phys. 96 (1992) 1.

16. W.C. Martin, R. Zalubas, and L. Hagan, "Atomic Energy Levels - Rare Earth Elements," Report No. NSRDS-NBS60; National Bureau of Standards; Washington, D.C., 1978.

17. R.W. Schwartz and P.N. Schatz, Phys. Rev. B 8 (1973) 3229.

18. The values of the Ce^{3+} 4f energy levels in Fig. 4 come from the electronic Raman results for $Cs_2NaCeCl_6$ given by H.-D. Amberger, G.G. Rosenbauer, and R.D. Fischer, J. Phys. Chem. Solids 38 (1977) 379.

19. K. Rajnak, E. Gamp, R. Shinomoto, and N. Edelstein, J. Chem. Phys. 80 (1984) 5942.

20. N. Edelstein, unpublished results.

21. J.-C. Krupa, Inorg. Chim. Acta 139 (1987) 223.

22. I.S. Poirot, W.K. Kot, N.M. Edelstein, M.M. Abraham, C.B. Finch, and L.A. Boatner, Phys. Rev. B 39 (1989) 6388.

23. W.T. Carnall, G.K. Liu, C.W. Williams, and M.F. Reid, J. Chem. Phys. 95 (1991) 7194.

24. W.T. Carnall, "A Systematic Analysis of the Spectra of Trivalent Actinide Chlorides in D_{3h} Site Symmetry," ANL 89/39.

25. W. Lukens and R.A. Andersen, private communication, 1992.

26. W.K. Kot, "Electronic Structure in the Actinides - Three Case Studies," LBL-30652, 1991.

27. B. Kanellakopulos, E. Dornberger, and F. Baumgartner, Inorg.Nucl. Chem. Lett. 10 (1974) 155.

28. J.W. Bruno, D.G. Kalina, E.A. Mintz, and T.J. Marks, J. Am. Chem. Soc. 104 (1982) 1860.

29. A.M. Koulkes-Pujo, J.F. Le Marechal, A. Dormond, and G. Folcher, Inorg. Chem. 26 (1987) 3171.

30. B.E. Bursten, L.F. Rhodes, and R.J. Strittmatter, J. Am. Chem. Soc. 111 (1989) 2756.

31. S.M. Beshouri, R.A. Andersen, N.M. Edelstein, W. Kot, P. Matsunaga, and A. Zalkin, Abstracts of Papers, 196th ACS National Meeting, American Chemical Society, Sept. 25-30, 1988, Inor 177.

32. S.D. Stults, "Tris(cyclopentadienyl)cerium and -Uranium: Relative Basicity, Structure, and Reactions," LBL-26124, 1988.

33. N. Edelstein, Eur. J. Solid State Inorg. Chem. 28 (1991) 47.

34. J. Meunier-Piret, J.P. Declercq, G. German, and M. van Meersche, Bull. Soc. Chim. Belg. 89 (1980) 121.

35. A.H.H. Chang and R.M. Pitzer, J. Am. Chem. Soc. 111 (1989) 2500.

	Pa^{4+}/Cs_2ZrCl_6 [4,5]		$(Et_4N)_2PaCl_6$ [9]		$(Et_4N)_2PaF_6$ [10]		Pa^{4+}/Cs_2ZrCl_6 [15,16]	
Energy Levels	Exp.	Calc.	Exp.	Calc.	Exp.	Calc.	Exp.	Calc.
6d $\Gamma_{8'g}$ (cm^{-1})							40000	40000
6d Γ_{7g} (cm^{-1})							23000	23000
6d Γ_{8g} (cm^{-1})							19954	19954
5f Γ_{6u} (cm^{-1})	8000	8121	8011	8029	11446	11537	8173	8215
5f $\Gamma_{8'u}$ (cm^{-1})	7085	6954	7022	6988	9708	9586	7272	7210
5f Γ_{7u} (cm^{-1})	5215	5215	5330	5347	5698	5717	5330	5413
5f Γ_{8u} (cm^{-1})		1912		1867		3708	2108	2133
5f Γ_{7u} (cm^{-1})	0	0	0	0	0	0	0	0
g values								
$g_{\Gamma_{7u}}$	|1.141|	-1.141		-1.115		-0.705	|1.141|	-0.979
Parameters								
B_0^4(5f)(cm^{-1})		7104		6665		14740		7244
B_0^6(5f))cm^{-1})		6708		394		1423		66.1
ζ_{5f} (cm^{-1})		1490		1523		1508		1511.2
B_0^4(6d)(cm^{-1})								39050
ζ_{6d} (cm^{-1})								1856.5
E_{Ave}(6d)(cm^{-1})								28582

Table 1. Spectroscopic data and fits for various Pa^{4+} octahedral systems.

Figure Captions

Figure 1. Schematic energy level diagram of Pa^{4+}/Cs_2ZrCl_6.

Figure 2. An absorption (5f → 6d) and an emission (6d → 5f) band of Pa^{4+}/Cs_2ZrCl_6. The continuous vertical lines at the bottom represent the 0-0 line and the a_{1g} progression of the $PaCl_6^{2-}$ complex. The long dashed lines and the short dashed lines show the features assigned to the t_{2g} and e_g vibrations, respectively. The data are plotted relative to the 0-0 line.

Figure 3. Energy level diagrams for the Pa^{4+} free ion, some Pa compounds, the Ce^{3+} free ion, and $Cs_2NaCeCl_6$. The arrows represent the energy differences between the centers of gravity of the f and d configurations.

Figure 4. EPR spectra of Cp_3"Th in methylcyclohexane (freezing point 147K) as a function of temperature. All data were obtained at 9.255 GHz.

Figure 5. Room temperature absorption spectrum of Cp_3"Th in methylcyclohexane (concentration = 7.8×10^{-4}M, pathlength 1 cm).

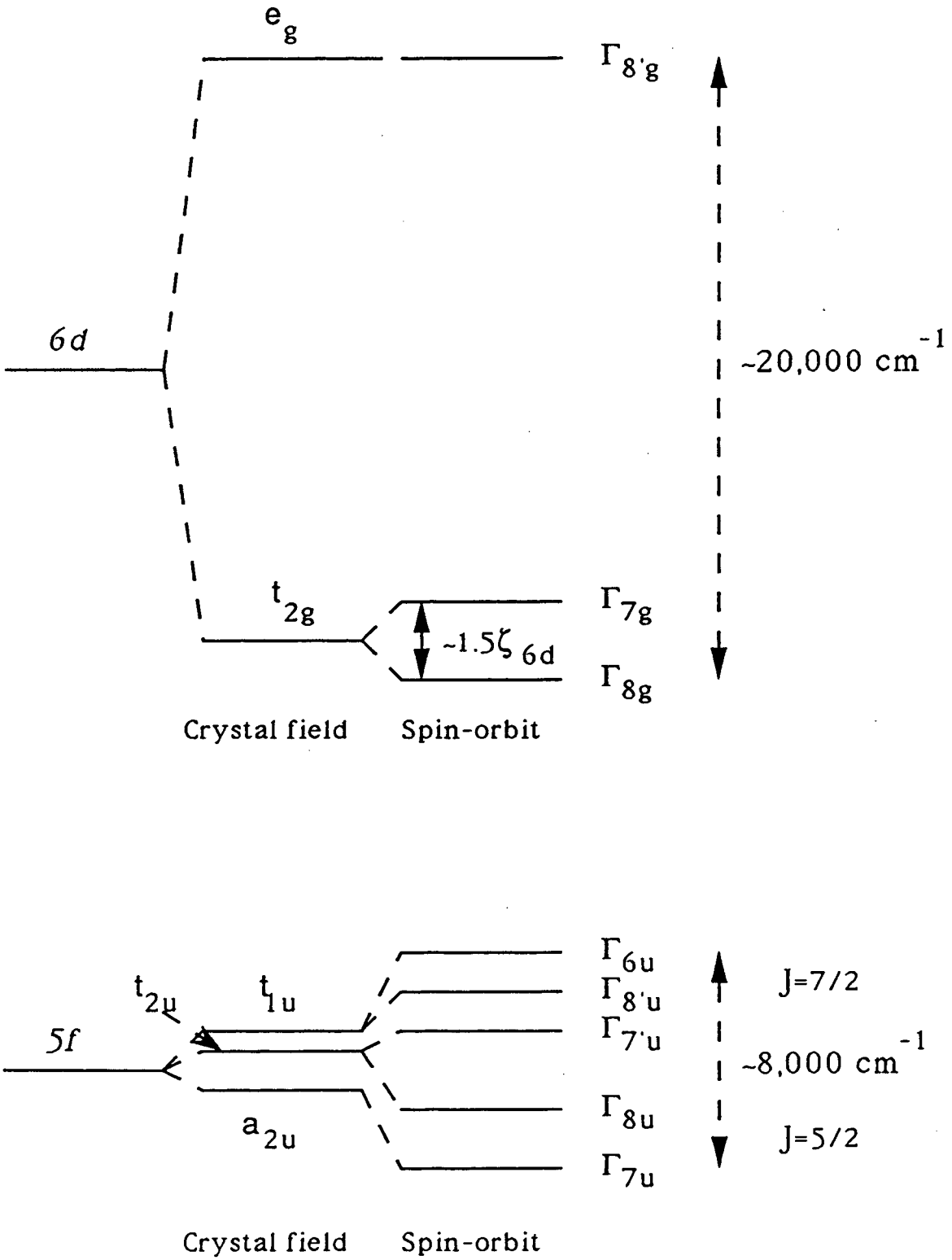
e_g
Γ_8'g
6d
~20,000 cm^-1
t_2g
Γ_7g
~1.5ζ_6d
Γ_8g
Crystal field
Spin-orbit
Γ_6u
Γ_8'u
Γ_7'u
Γ_8u
Γ_7u
t_2u
t_1u
5f
a_2u
J=7/2
~8,000 cm^-1
J=5/2
Crystal field
Spin-orbit

Figure 1

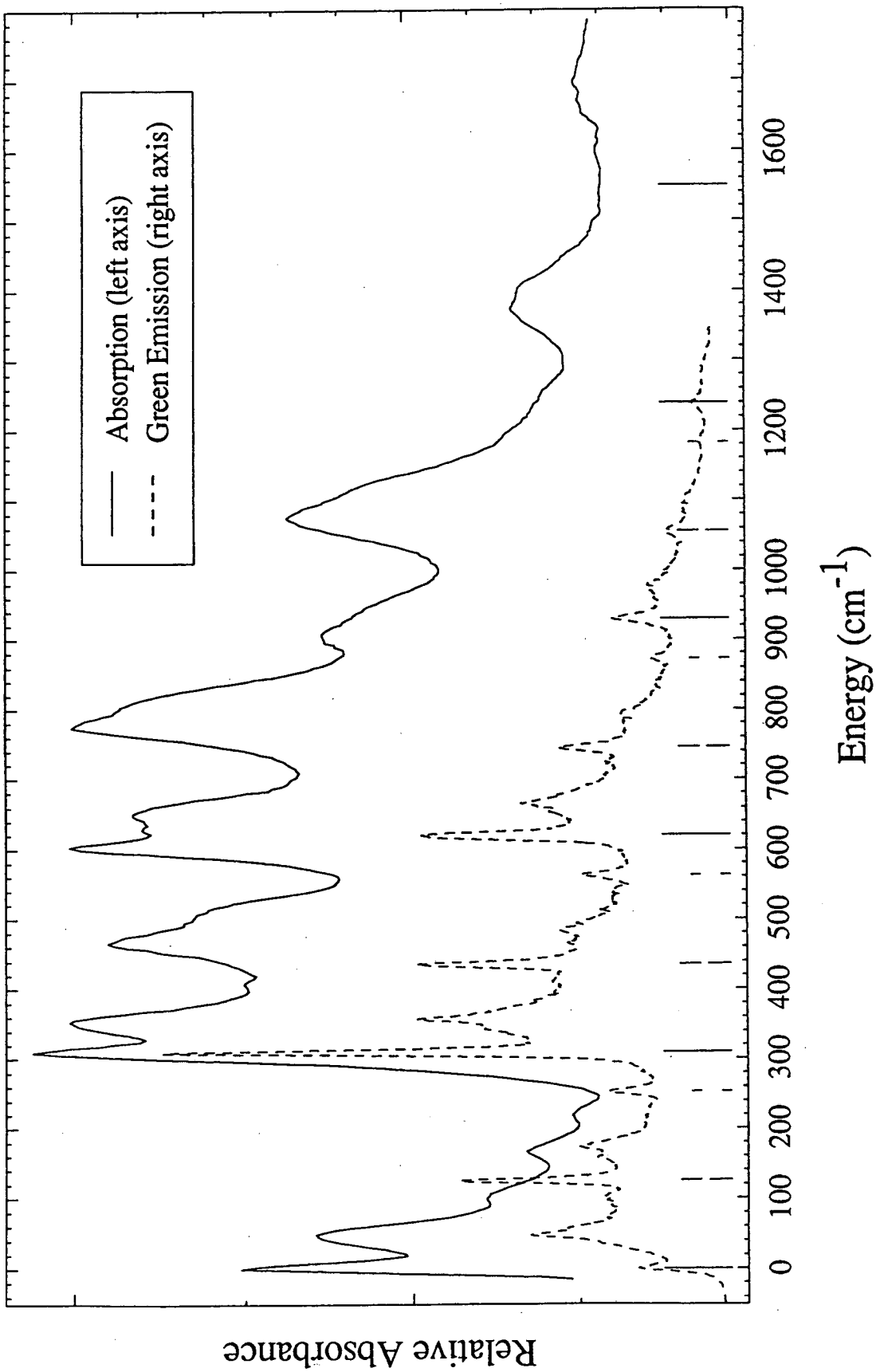
Relative Emission
Absorption (left axis)
Green Emission (right axis)
Relative Absorbance
0
100
200
300
400
500
600
700
800
900
1000
1200
1400
1600
Energy (cm-1)

Figure 2

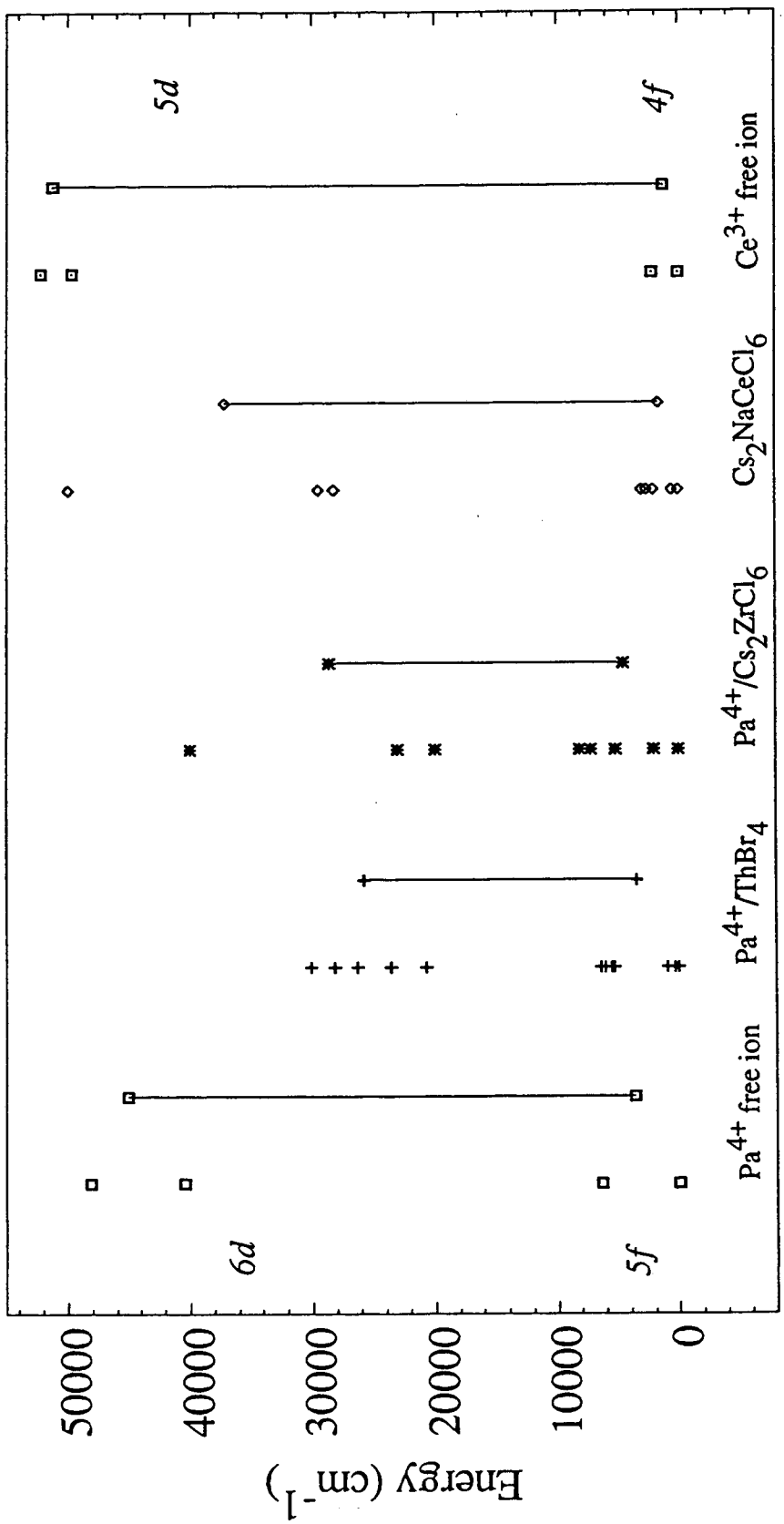
Pa4+ and Ce3+ Energy Levels
Energy (cm-1)
50000
40000
30000
20000
10000
0
6d
5f
5d
4f
Pa4+ free ion
Pa4+/ThBr4
Pa4+/Cs2ZrCl6
Cs2NaCeCl6
Ce3+ free ion

Figure 3

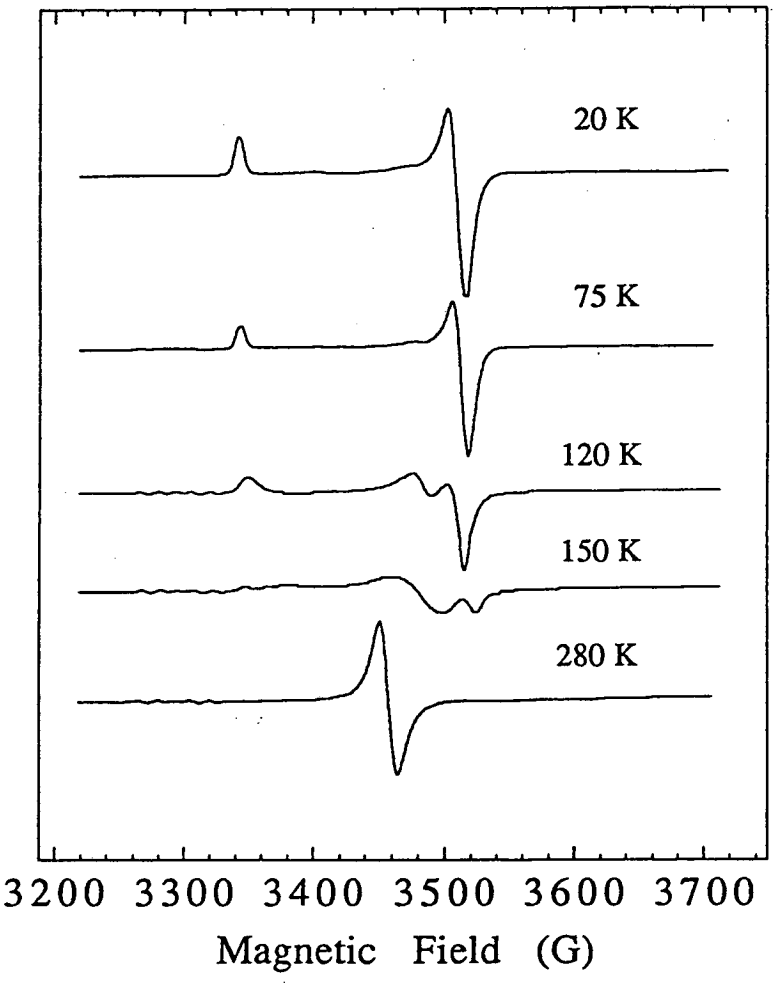
20 K
75 K
120 K
150 K
280 K
3200 3300 3400 3500 3600 3700
Magnetic Field (G)

Figure 4

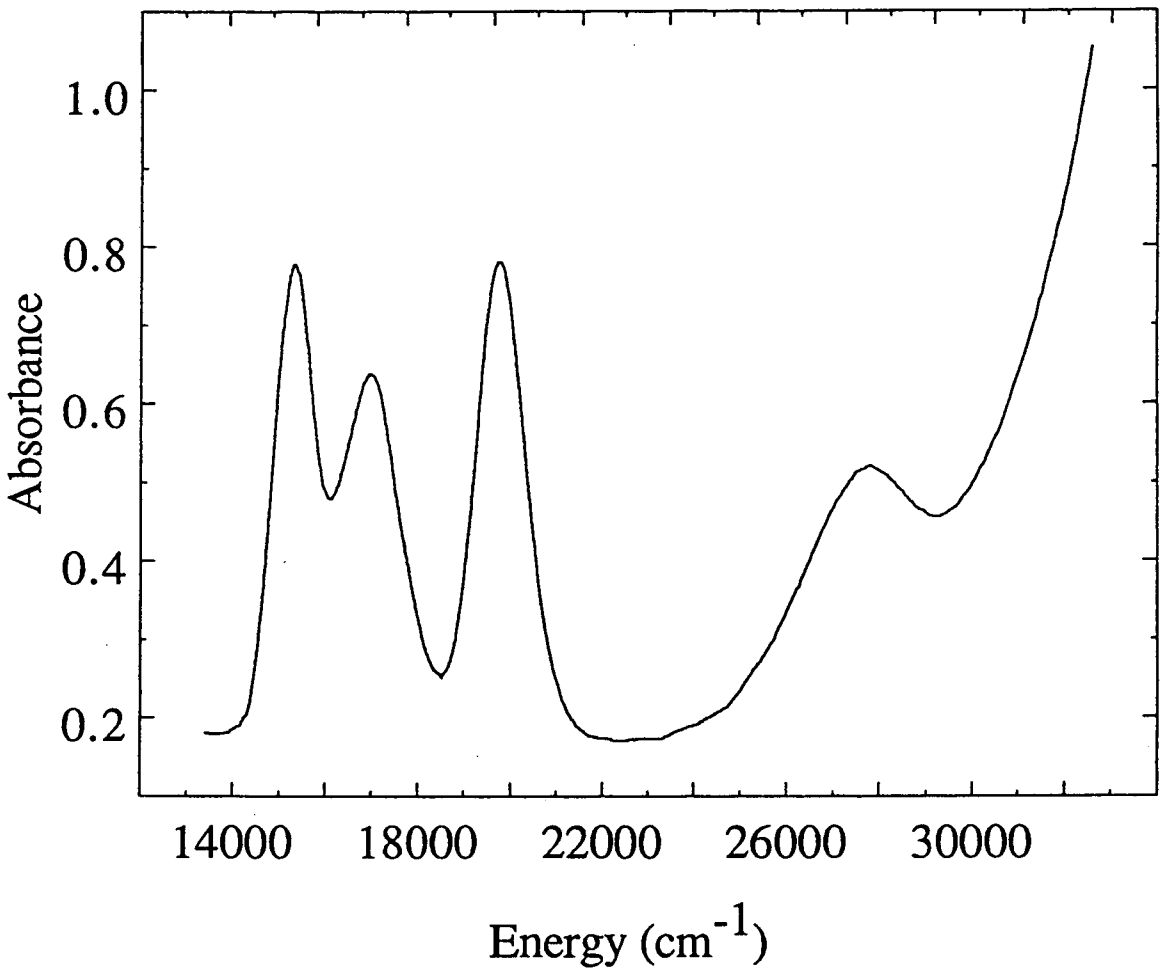
1.0
0.8
0.6
0.4
0.2
Absorbance
14000
18000
22000
26000
30000
Energy (cm-1)

Figure 5

LAWRENCE BERKELEY LABORATORY
UNIVERSITY OF CALIFORNIA
TECHNICAL INFORMATION DEPARTMENT
BERKELEY, CALIFORNIA 94720